Science Advances
AAAS

Supplementary Materials for

Autophagy supports mitochondrial metabolism through the regulation of iron homeostasis in pancreatic cancer

Subhadip Mukhopadhyay *et al.*

Corresponding author: Alec C. Kimmelman, alec.kimmelman@nyulangone.org

Sci. Adv. **9**, eadf9284 (2023)
DOI: 10.1126/sciadv.adf9284

This PDF file includes:

Supplementary Figures

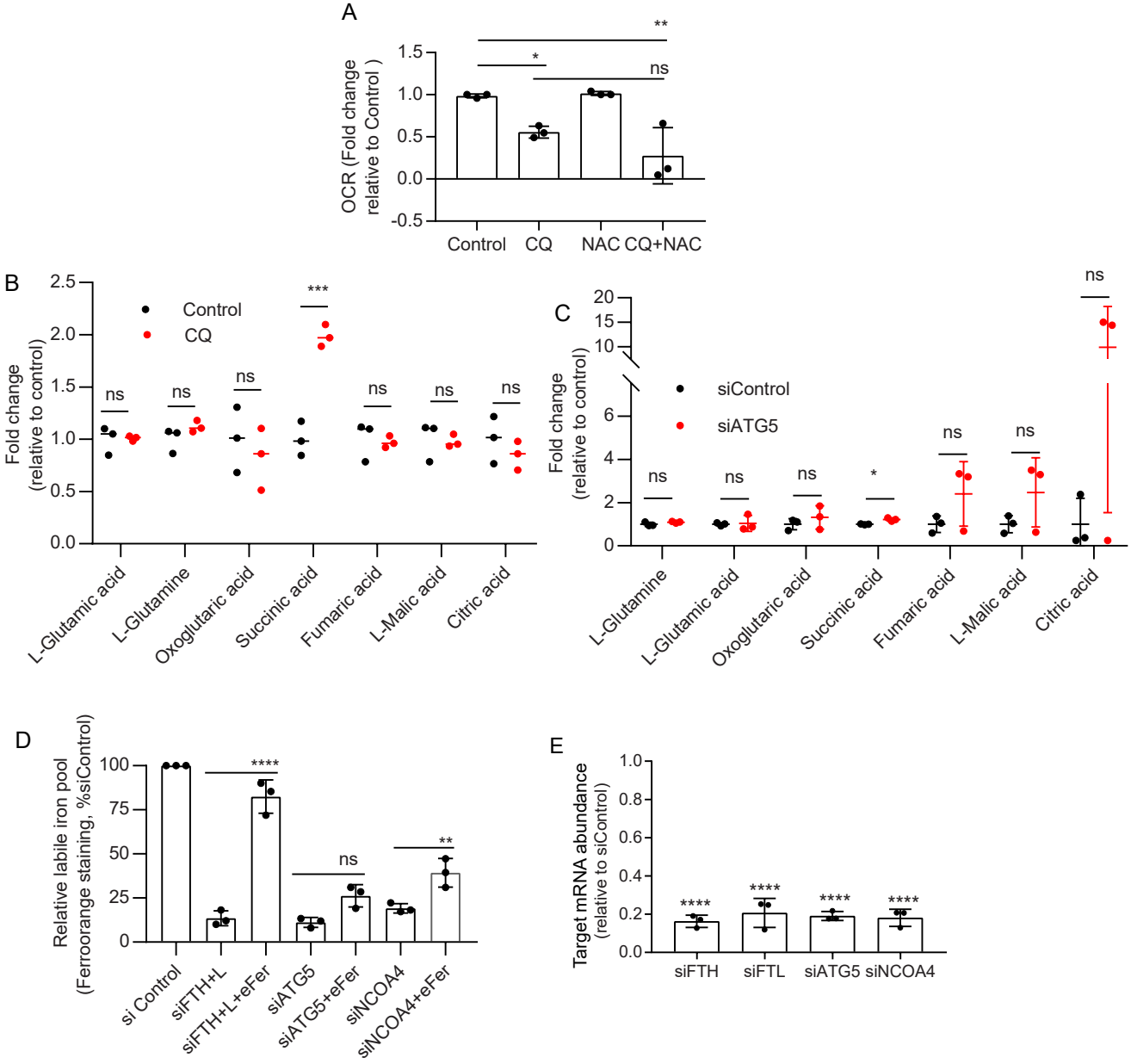

Fig.S1: Analysis of OCR, metabolomics, and the labile iron pool after autophagy inhibition in PDAC. (A) CQ treated PDAC cells are supplemented with NAC and OCR is measured from n=3 (Statistical analysis done using One way ANOVA Holm Sidak's test). PDAC cells treated with CQ (B) or siATG5 (C) were analyzed for TCA substrates by LC-MS. Statistical analysis done using unpaired two-tailed t-tests. This data includes the same succinate levels that were shown in Fig2D. (D) Equine ferritin (1mg/ml, 8h) was added to cells under autophagy or ferritinophagy inhibited conditions, and the LIP level was determined. (E) mRNA level was measured by qRT-PCR after siRNA against indicated target genes were used in PDAC cells. Data are mean ±s.d and *P* values were quantified using one way ANOVA with Tukey's post hoc test. ****$P < 0.0001$, ***$P < 0.001$, **$P < 0.01$, * $P < 0.05$ were considered as significant.

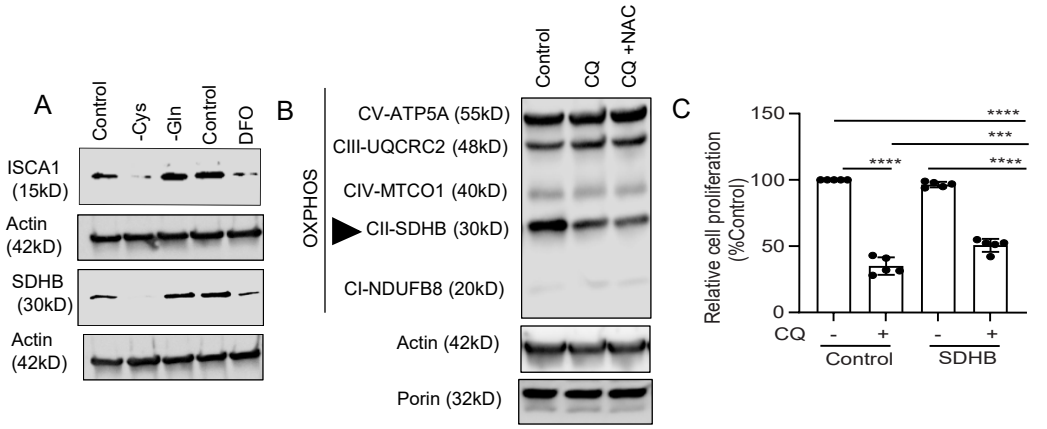

Fig.S2: Protein expression of the Fe-S protein SDHB cannot be rescued by NAC supplementation during autophagy loss in PDAC. (A) 8988T PDAC cells were either starved for cystine (glutamine starvation was used as a random amino acid starvation control) or exposed to iron chelation, followed by western blotting for indicated proteins. (B) OXPHOS, VDAC1 (porin) protein levels were measured by immunoblot upon co-treatment with CQ and NAC. SDHB is indicated in (B) using a triangle. (C) PDAC expressing control or SDHB overexpressing cells were treated with CQ, followed by an analysis of their cell proliferation. Data are mean ±s.d and *P* values were quantified using one-way ANOVA with Tukey's post hoc test. ****$P < 0.0001$, ***$P < 0.001$, **$P < 0.01$ were considered as significant.

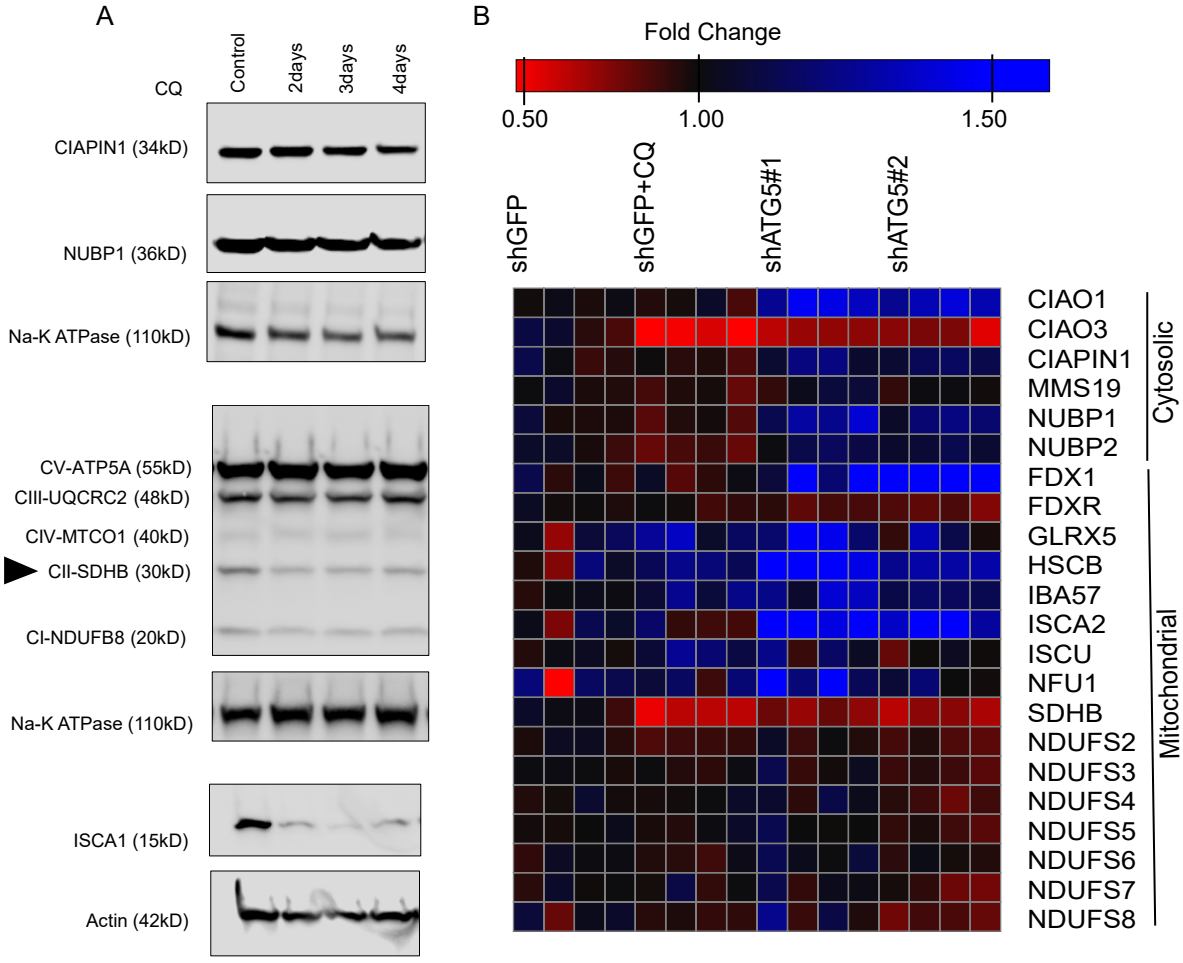

Fig.S3: Analysis of mitochondrial and cytoplasmic Fe-S cluster proteins by immunoblotting and proteomics. (A) 8988T cells were treated for indicated timepoints and immunoblotted for cytoplasmic, mitochondrial Fe-S proteins. (B) Heatmap showing quantiative proteomics analysis of mitochondrial and cytoplasmic Fe-S cluster proteins from autophagy inhibited 8988T cells. Statiscal analysis of Fig.S3B is shown in following Supplementary Table-1.

Supplementary Table-1: Two way ANOVA Tukey's multiple comparison with the statistical summary and adjusted *P* value for Fig.S3B

CIAO1		
shGFP vs. shGFP+CQ	ns	0.9733
shGFP vs. shATG5#1	****	<0.0001
shGFP vs. shATG5#2	****	<0.0001
CIAO3		
shGFP vs. shGFP+CQ	****	<0.0001
shGFP vs. shATG5#1	***	0.0008
shGFP vs. shATG5#2	**	0.0013
CIAPIN1		
shGFP vs. shGFP+CQ	ns	0.879
shGFP vs. shATG5#1	ns	0.1775
shGFP vs. shATG5#2	ns	0.2947
MMS19		
shGFP vs. shGFP+CQ	ns	0.6599
shGFP vs. shATG5#1	ns	0.9619
shGFP vs. shATG5#2	ns	0.9953
NUBP1		
shGFP vs. shGFP+CQ	ns	0.6593
shGFP vs. shATG5#1	**	0.0016
shGFP vs. shATG5#2	ns	0.0966
NUBP2		
shGFP vs. shGFP+CQ	ns	0.2244
shGFP vs. shATG5#1	ns	0.5099
shGFP vs. shATG5#2	ns	0.6289
FDX1		
shGFP vs. shGFP+CQ	ns	0.9643
shGFP vs. shATG5#1	****	<0.0001
shGFP vs. shATG5#2	****	<0.0001
FDXR		
shGFP vs. shGFP+CQ	ns	0.9247
shGFP vs. shATG5#1	ns	0.4248
shGFP vs. shATG5#2	ns	0.1264
GLRX5		
shGFP vs. shGFP+CQ	*	0.0185
shGFP vs. shATG5#1	****	<0.0001
shGFP vs. shATG5#2	ns	0.6029
HSCB		
shGFP vs. shGFP+CQ	ns	0.0525
shGFP vs. shATG5#1	****	<0.0001
shGFP vs. shATG5#2	***	0.0006
IBA57		
shGFP vs. shGFP+CQ	ns	0.0962
shGFP vs. shATG5#1	**	0.0022
shGFP vs. shATG5#2	ns	0.1836

ISCA2		
shGFP vs. shGFP+CQ	ns	0.9864
shGFP vs. shATG5#1	****	<0.0001
shGFP vs. shATG5#2	****	<0.0001
ISCU		
shGFP vs. shGFP+CQ	ns	0.108
shGFP vs. shATG5#1	ns	0.5647
shGFP vs. shATG5#2	ns	0.9622
NFU1		
shGFP vs. shGFP+CQ	ns	0.6067
shGFP vs. shATG5#1	****	<0.0001
shGFP vs. shATG5#2	ns	0.7728
SDHB		
shGFP vs. shGFP+CQ	****	<0.0001
shGFP vs. shATG5#1	*	0.0132
shGFP vs. shATG5#2	***	0.0007
NDUFS2		
shGFP vs. shGFP+CQ	ns	0.5599
shGFP vs. shATG5#1	ns	0.9946
shGFP vs. shATG5#2	ns	0.4575
NDUFS3		
shGFP vs. shGFP+CQ	ns	0.9908
shGFP vs. shATG5#1	ns	0.9947
shGFP vs. shATG5#2	ns	0.5696
NDUFS4		
shGFP vs. shGFP+CQ	ns	0.9996
shGFP vs. shATG5#1	ns	0.9552
shGFP vs. shATG5#2	ns	0.4563
NDUFS5		
shGFP vs. shGFP+CQ	ns	>0.9999
shGFP vs. shATG5#1	ns	0.9688
shGFP vs. shATG5#2	ns	0.6388
NDUFS6		
shGFP vs. shGFP+CQ	ns	0.9348
shGFP vs. shATG5#1	ns	0.8049
shGFP vs. shATG5#2	ns	0.9871
NDUFS7		
shGFP vs. shGFP+CQ	ns	0.9995
shGFP vs. shATG5#1	ns	0.9858
shGFP vs. shATG5#2	ns	0.3656
NDUFS8		
shGFP vs. shGFP+CQ	ns	0.8723
shGFP vs. shATG5#1	ns	0.8307
shGFP vs. shATG5#2	ns	0.1861

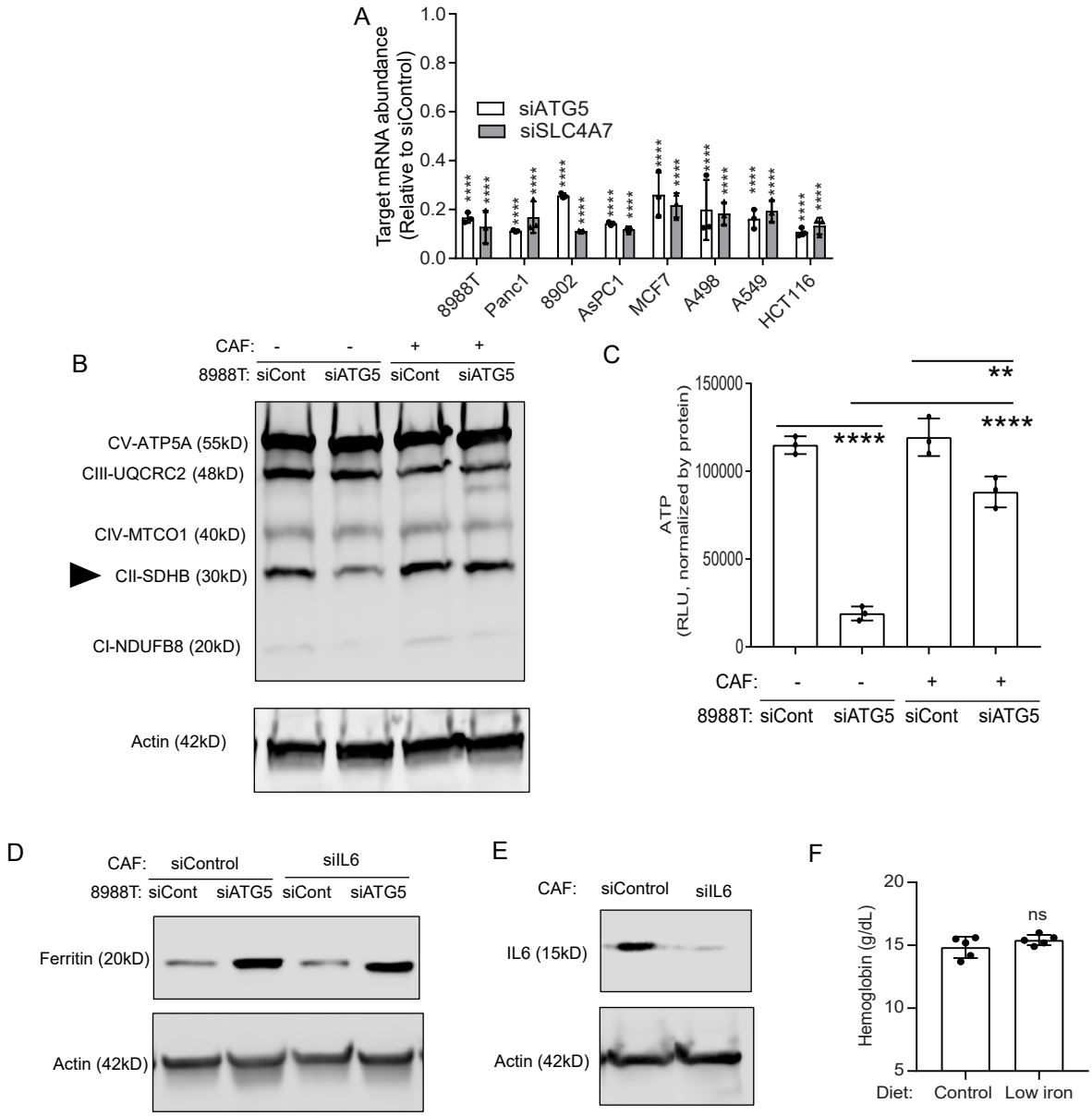

Fig.S4: CAFs rescue SDHB levels in autophagy impaired PDAC and undergo paracrine signaling to regulate the IL6-ferritin axis. (A) siRNA knockdown quality of indicated genes were analyzed by mRNA level quantification. These knockdown cells were used in Fig.7B. (B) Western blot analysis of OXPHOS cocktail was performed in autophagy intact or inhibited PDAC lysates which was mono or co-cultured with CAFs. (C) Cell lysates from conditions similar in (B) was used for quantification of PDAC ATP. (D) CAFs with or without IL6 knocked down were cocultured with PDAC having ATG5 inhibition and the CAF lysates were used for ferritin immunoblots. (E) IL6 was knocked down in CAF and the lysates were immunoblotted for IL6. (F) Hemoglobin analysis of B6 mice fed on indicated diet for 1 month was analyzed using retroorbital blood by Hemavet analyzer. Data are mean ±s.d and *P* values were quantified using one-way ANOVA with Tukey's post hoc test. ****$P < 0.0001$, ***$P < 0.001$, **$P < 0.01$ were considered as significant.

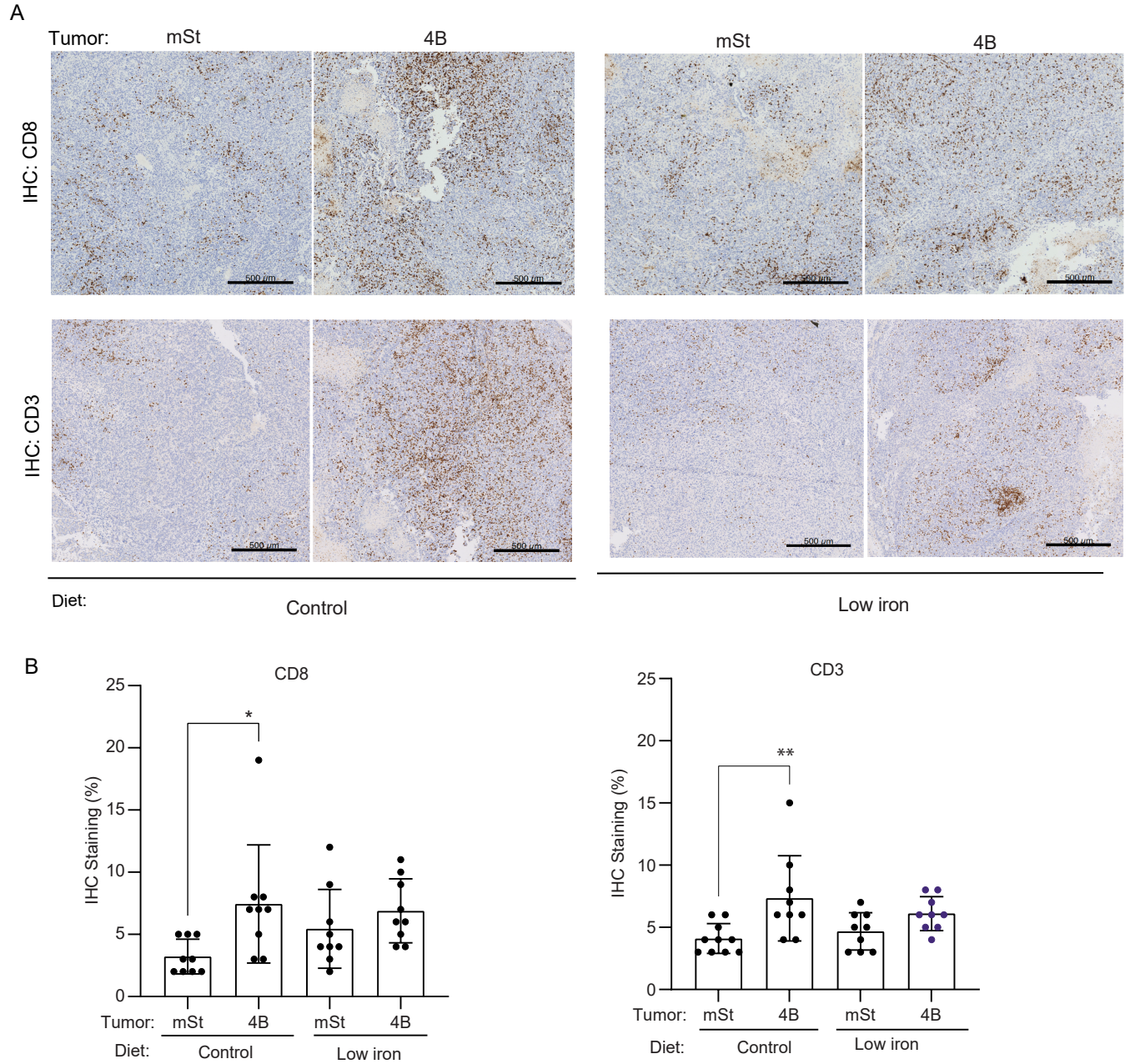

Fig.S5: Iron restriction does not further enhance immune infiltration in the setting of autophagy inhibition. (A) Immunohistochemical analysis was performed for CD8 and CD3 using tumor samples from Fig.10A followed by their quantification in (B). Data are mean ±s.d and *P* values were quantified using one-way ANOVA with Tukey's post hoc test. ****$P < 0.0001$, ***$P < 0.001$, **$P < 0.01$, *$P < 0.05$ were considered as significant.

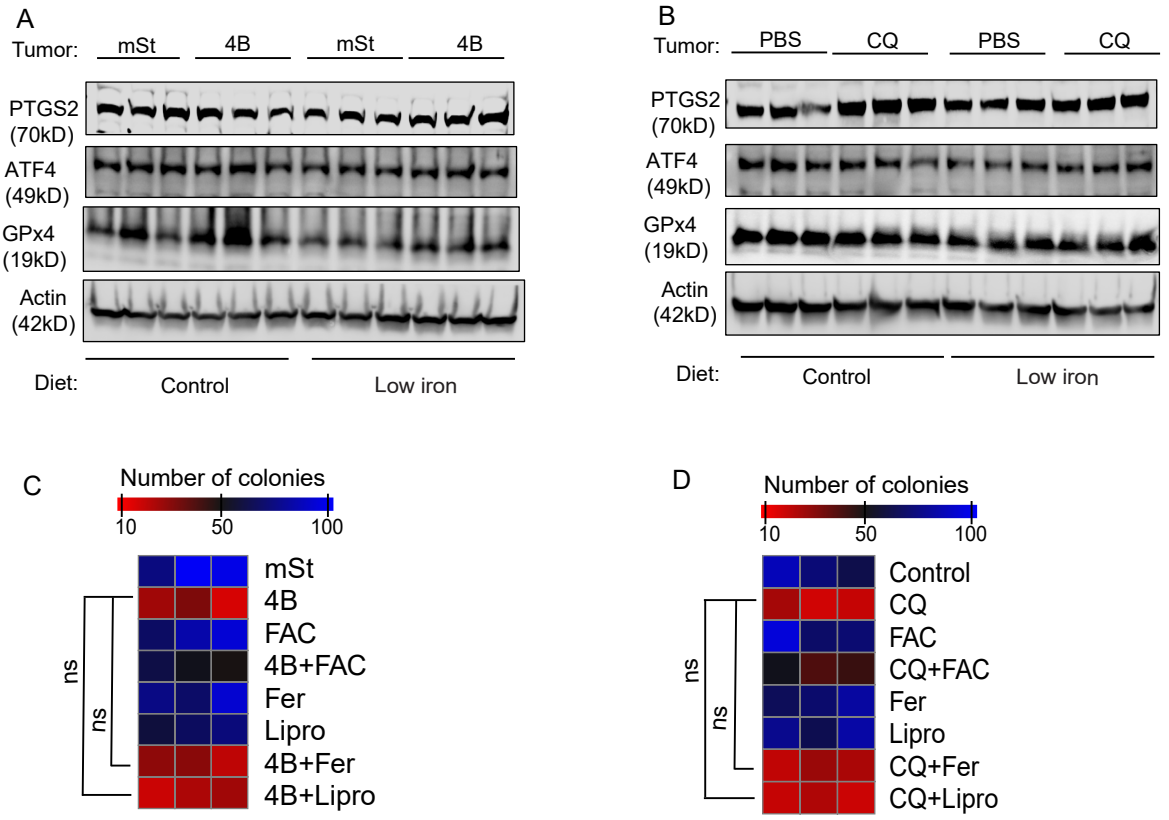

Fig.S6: Proliferative inhibition in PDAC by loss of autophagy does not involve ferroptosis. Indicated ferroptosis markers were analyzed from tumor samples (from Fig.10) bearing autophagy inhibition by Atg4Bdn (A) or CQ (B)with or without low iron diet by immunoblotting. Autophagy was inhibited in HY19636 PDAC cells by Atg4Bdn (C) or CQ (D) and the colony formation assay was enumerated after treating the cells with Ferrostatin-1 (20μM) or Liproxstatin-1 (14μM). *P* values were quantified using one way ANOVA with Tukey's post hoc test and $P>0.05$ were considered as non-significant (ns).

Supplementary Methods:

Histology and immunohistochemistry: The Experimental Pathology Research Laboratory at NYU Grossman School of Medicine carried out staining for hematoxylin and eosin, CD8 (Cell Signaling Technology, 98941S), CD3 (Cell Signaling Technology, 78588S) and slide scanning on the tumor tissues was done after they had been fixed in formalin overnight and embedded in paraffin. IHC images were quantified using Leica Biosystems Aperio ImageScope software; necrotic and non-tumor regions were excluded from the analysis.

Quantitative Proteomics: Analysis of quantitative proteomics on PaTu-8988T cell lines was performed as previously described (33) after inhibiting autophagy genetically using shRNAs against ATG5 or pharmacologically using CQ. Proteins were extracted using a lysis buffer composed of 8 M urea, 200 mM EPPS (pH 8.5), supplemented with protease inhibitors. Around 50-100μg of protein extracts underwent reduction, alkylation followed by precipitation. These protein pellets were digested and 50μg of peptides were labelled with TMT reagent. Protein loading was equalized by checking ratio of 2μg of each TMT-labeled sample. Sample fractionation was done using basic pH RP-HPLC. Desalted samples were analyzed by LC-MS/MS/MS. Data acquisition was performed with Orbitrap Lumos mass spectrometer in-line with a Proxeon NanoLC-1200 UHPLC system followed by processing with Comet (34) and a previously reported informatics pipeline (35). Spectral searches were performed using FASTA-formatted databases (Uniprot Human, 2020). Protein quantitative values were normalized to ensure the sum of all protein signals in every channel was equalized to account for sample loading.

REFERENCES AND NOTES

1. R. L. Siegel, K. D. Miller, H. E. Fuchs, A. Jemal, Cancer statistics, 2021. *CA Cancer J. Clin.* **71**, 7–33 (2021).

2. L. Rahib, B. D. Smith, R. Aizenberg, A. B. Rosenzweig, J. M. Fleshman, L. M. Matrisian, Projecting cancer incidence and deaths to 2030: The unexpected burden of thyroid, liver, and pancreas cancers in the United States. *Cancer Res.* **74**, 2913–2921 (2014).

3. S. Yang, X. Wang, G. Contino, M. Liesa, E. Sahin, H. Ying, A. Bause, Y. Li, J. M. Stommel, G. Dell'antonio, J. Mautner, G. Tonon, M. Haigis, O. S. Shirihai, C. Doglioni, N. Bardeesy, A. C. Kimmelman, Pancreatic cancers require autophagy for tumor growth. *Genes Dev.* **25**, 717–729 (2011).

4. A. Yang, N. V. Rajeshkumar, X. Wang, S. Yabuuchi, B. M. Alexander, G. C. Chu, D. D. Von Hoff, A. Maitra, A. C. Kimmelman, Autophagy is critical for pancreatic tumor growth and progression in tumors with p53 alterations. *Cancer Discov.* **4**, 905–913 (2014).

5. C. M. Sousa, D. E. Biancur, X. Wang, C. J. Halbrook, M. H. Sherman, L. Zhang, D. Kremer, R. F. Hwang, A. K. Witkiewicz, H. Ying, J. M. Asara, R. M. Evans, L. C. Cantley, C. A. Lyssiotis, A. C. Kimmelman, Pancreatic stellate cells support tumour metabolism through autophagic alanine secretion. *Nature* **536**,479–483 (2016).

6. K. Yamamoto, A. Venida, J. Yano, D. E. Biancur, M. Kakiuchi, S. Gupta, A. S. W. Sohn, S. Mukhopadhyay, E. Y. Lin, S. J. Parker, R. S. Banh, J. A. Paulo, K. W. Wen, J. Debnath, G. E. Kim, J. D. Mancias, D. T. Fearon, R. M. Perera, A. C. Kimmelman, Autophagy promotes immune evasion of pancreatic cancer by degrading MHC-I. *Nature* **581**,100–105 (2020).

7. H. J. Zeh, N. Bahary, B. A. Boone, A. D. Singhi, J. L. Miller-Ocuin, D. P. Normolle, A. H. Zureikat, M. E. Hogg, D. L. Bartlett, K. K. Lee, A. Tsung, J. W. Marsh, P. Murthy, D. Tang, N. Seiser, R. K. Amaravadi, V. Espina, L. Liotta, M. T. Lotze, A randomized phase II preoperative study of autophagy inhibition with high-dose hydroxychloroquine and gemcitabine/nab-paclitaxel in pancreatic cancer patients. *Clin. Cancer Res.* **26**, 3126–3134 (2020).

8. J. D. Mancias, X. Wang, S. P. Gygi, J. W. Harper, A. C. Kimmelman, Quantitative proteomics identifies NCOA4 as the cargo receptor mediating ferritinophagy. *Nature* **509**, 105–109 (2014).

9. R. A. Weber, F. S. Yen, S. P. V. Nicholson, H. Alwaseem, E. C. Bayraktar, M. Alam, R. C. Timson, K. La, M. Abu-Remaileh, H. Molina, K. Birsoy, Maintaining iron homeostasis is the key role of lysosomal acidity for cell proliferation. *Mol. Cell* **77**, 645–655.e7.(2020).

10. F. Rizzollo, S. More, P. Vangheluwe, P. Agostinis, The lysosome as a master regulator of iron metabolism. *Trends Biochem. Sci.* **46**, 960–975 (2021).

11. K. F. Yambire, C. Rostosky, T. Watanabe, D. Pacheu-Grau, S. Torres-Odio, A. Sanchez-Guerrero, O. Senderovich, E. G. Meyron-Holtz, I. Milosevic, J. Frahm, A. P. West, N. Raimundo, Impaired lysosomal acidification triggers iron deficiency and inflammation in vivo. *eLife* **8**, e51031 (2019).

12. S. Mukhopadhyay, D. E. Biancur, S. J. Parker, K. Yamamoto, R. S. Banh, J. A. Paulo, J. D. Mancias, A. C. Kimmelman, Autophagy is required for proper cysteine homeostasis in pancreatic cancer through regulation of SLC7A11. *Proc. Natl. Acad. Sci. U.S.A.* **118**, e2021475118 (2021).

13. E. Szarek, E. R. Ball, A. Imperiale, M. Tsokos, F. R. Faucz, A. Giubellino, F. M. Moussallieh, I. J. Namer, M. S. Abu-Asab, K. Pacak, D. Taïeb, J. A. Carney, C. A. Stratakis, Carney triad, SDH-deficient tumors, and $Sdhb^{+/-}$ mice share abnormal mitochondria. *Endocr. Relat. Cancer* **22**, 345–352 (2015).

14. L. K. Beilschmidt, S. Ollagnier de Choudens, M. Fournier, I. Sanakis, M. A. Hograindleur, M. Clémancey, G. Blondin, S. Schmucker, A. Eisenmann, A. Weiss, P. Koebel, N. Messaddeq, H. Puccio, A. Martelli, ISCA1 is essential for mitochondrial Fe_4S_4 biogenesis in vivo. *Nat. Commun.* **8**, 15124 (2017).

15. A. Torraco, O. Stehling, C. Stümpfig, R. Rösser, D. De Rasmo, G. Fiermonte, D. Verrigni, T. Rizza, A. Vozza, M. Di Nottia, D. Diodato, D. Martinelli, F. Piemonte, C. Dionisi-Vici, E.

Bertini, R. Lill, R. Carrozzo, ISCA1 mutation in a patient with infantile-onset leukodystrophy causes defects in mitochondrial [4Fe-4S] proteins. *Hum. Mol. Genet.* **27**, 2739–2754 (2018).

16. J. Encarnación-Rosado, A. C. Kimmelman, Harnessing metabolic dependencies in pancreatic cancers. *Nat. Rev. Gastroenterol. Hepatol.* **18**, 482–492 (2021).

17. B. M. Wolpin, D. A. Rubinson, X. Wang, J. A. Chan, J. M. Cleary, P. C. Enzinger, C. S. Fuchs, N. J. McCleary, J. A. Meyerhardt, K. Ng, D. Schrag, A. L. Sikora, B. A. Spicer, L. Killion, H. Mamon, A. C. Kimmelman, Phase II and pharmacodynamic study of autophagy inhibition using hydroxychloroquine in patients with metastatic pancreatic adenocarcinoma. *Oncologist* **19**,637–638 (2014).

18. E. Nemeth, M. S. Tuttle, J. Powelson, M. B. Vaughn, A. Donovan, D. M. Ward, T. Ganz, J. Kaplan, Hepcidin regulates cellular iron efflux by binding to ferroportin and inducing its internalization. *Science* **306**,2090–2093 (2004).

19. J. T. Rogers, Ferritin translation by interleukin-1and interleukin-6: The role of sequences upstream of the start codons of the heavy and light subunit genes. *Blood* **87**, 2525–2537 (1996).

20. M. Kobune, Y. Kohgo, J. Kato, E. Miyazaki, Y. Niitsu, Interleukin-6 enhances hepatic transferrin uptake and ferritin expression in rats. *Hepatology* **19**, 1468–1475 (1994).

21. F. Richard, J. J. van Lier, B. Roubert, T. Haboubi, U. M. Göhring, F. Dürrenberger, Oral ferroportin inhibitor VIT-2763: First-in-human, phase 1 study in healthy volunteers. *Am. J. Hematol.* **95**, 68–77 (2020).

22. V. Manolova, N. Nyffenegger, A. Flace, P. Altermatt, A. Varol, C. Doucerain, H. Sundstrom, F. Dürrenberger. Oral ferroportin inhibitor ameliorates ineffective erythropoiesis in a model of β-thalassemia. *J. Clin. Invest.* **130**, 491–506 (2019).

23. C. A. Lyssiotis, A. C. Kimmelman, Metabolic interactions in the tumor microenvironment. *Trends Cell Biol.* **27**, 863–875 (2017).

24. S. J. Parker, C. R. Amendola, K. E. R. Hollinshead, Q. Yu, K. Yamamoto, J. Encarnación-Rosado, R. E. Rose, M. M. LaRue, A. S. W. Sohn, D. E. Biancur, J. A. Paulo, S. P. Gygi, D. R. Jones, H. Wang, M. R. Philips, D. Bar-Sagi, J. D. Mancias, A. C. Kimmelman, Selective alanine transporter utilization creates a targetable metabolic niche in pancreatic cancer. *Cancer Discov.* **10**, 1018–1037 (2020).

25. R. S. Banh, D. E. Biancur, K. Yamamoto, A. S. W. Sohn, B. Walters, M. Kuljanin, A. Gikandi, H. Wang, J. D. Mancias, R. J. Schneider, M. E. Pacold, A. C. Kimmelman, Neurons release serine to support mRNA translation in pancreatic cancer. *Cell* **183**, 1202–1218.e25. (2020).

26. N. Santana-Codina, M. Q. Del Rey, K. S. Kapner, H. Zhang, A. Gikandi, C. Malcolm, C. Poupault, M. Kuljanin, K. M. John, D. E. Biancur, B. Chen, N. K. Das, K. E. Lowder, C. J. Hennessey, W. Huang, A. Yang, Y. M. Shah, J. A. Nowak, A. J. Aguirre, J. D. Mancias, NCOA4-mediated ferritinophagy is a pancreatic cancer dependency via maintenance of iron bioavailability for iron-sulfur cluster proteins. *Cancer Discov.* **12**, 2180–2197 (2022).

27. R. Lock, C. M. Kenific, A. M. Leidal, E. Salas, J. Debnath, Autophagy-dependent production of secreted factors facilitates oncogenic RAS-driven invasion. *Cancer Discov.* **4**,466–479 (2014).

28. M. Ravichandran, J. Hu, C. Cai, N. P. Ward, A. Venida, C. Foakes, M. Kuljanin, A. Yang, C. J. Hennessey, Y. Yang, B. R. Desousa, G. Rademaker, A. A. L. Staes, Z. Cakir, I. H. Jain, A. J. Aguirre, J. D. Mancias, Y. Shen, G. M. DeNicola, R. M. Perera, Coordinated transcriptional and catabolic programs support iron-dependent adaptation to RAS-MAPK pathway inhibition in pancreatic cancer. *Cancer Discov.* **12**, 2198–2219 (2022).

29. M. N. Sutton, S. T. Gammon, R. Muzzioli, F. Pisaneschi, B. Radaram, P. Yang, D. Piwnica-Worms, RAS-driven macropinocytosis of albumin or dextran reveals mutation-specific target engagement of RAS p.G12C inhibitor ARS-1620 by NIR-fluorescence imaging. *Mol. Imaging Biol.* **24**, 498–509 (2022).

30. V. Wilkens, W. Kohl, K. Busch, Restricted diffusion of OXPHOS complexes in dynamic mitochondria delays their exchange between cristae and engenders a transitory mosaic distribution. *J. Cell Sci.* **126**, 103–116 (2013).

31. K. E. R. Hollinshead, S. J. Parker, V. V. Eapen, J. Encarnacion-Rosado, A. Sohn, T. Oncu, M. Cammer, J. D. Mancias, A. C. Kimmelman, Respiratory supercomplexes promote mitochondrial efficiency and growth in severely hypoxic pancreatic cancer. *Cell Rep.* **33**, 108231 (2020).

32. S. J. Parker, J. Encarnación-Rosado, K. E. R. Hollinshead, D. M. Hollinshead, L. J. Ash, J. A. K. Rossi, E. Y. Lin, A. S. W. Sohn, M. R. Philips, D. R. Jones, A. C. Kimmelman, Spontaneous hydrolysis and spurious metabolic properties of α-ketoglutarate esters. *Nat. Commun.* **12**, 4905 (2021).

33. N. Santana-Codina, A. S. Chandhoke, Q. Yu, B. Małachowska, M. Kuljanin, A. Gikandi, M. Stańczak, S. Gableske, M. P. Jedrychowski, D. A. Scott, A. J. Aguirre, W. Fendler, N. S. Gray, J. D. Mancias, Defining and targeting adaptations to oncogenic KRASG12C inhibition using quantitative temporal proteomics. *Cell Rep.* **30**, 4584–4599.e4. (2020).

34. J. K. Eng, M. R. Hoopmann, T. A. Jahan, J. D. Egertson, W. S. Noble, M. J. MacCoss, A deeper look into Comet—Implementation and features. *J. Am. Soc. Mass Spectrom.* **11**, 1865–1874 (2015).

35. G. C. McAlister, D. P. Nusinow, M. P. Jedrychowski, M. Wühr, E. L. Huttlin, B. K. Erickson, R. Rad, W. Haas, S. P. Gygi, MultiNotch MS_3 enables accurate, sensitive, and multiplexed detection of differential expression across cancer cell line proteomes. *Anal. Chem.* **86**, 7150–8 (2014).